Materials Research Bulletin 88 (2017) 174–181

Contents lists available at ScienceDirect

Materials Research Bulletin

journal homepage: www.elsevier.com/locate/matresbu

# Crystal structure and microwave dielectric properties of new alkaline earth vanadate $A_4V_2O_9$ (A = Ba, Sr, Ca, Mg and Zn) ceramics for LTCC applications

Avanoor Neelakantan Unnimaya, Elattuvalappil Kalathil Suresh, Ravendran Ratheesh*,[1]

*Microwave Materials Group, Centre for Materials for Electronics Technology (C-MET), Ministry of Electronics and Information Technology, Government of India, Athani P.O, Thrissur, Kerala 680581, India*

ARTICLE INFO

*Article history:*
Received 5 October 2016
Received in revised form 1 December 2016
Accepted 22 December 2016
Available online 23 December 2016

*Keywords:*
A. Ceramics
B. Microstructure
C. X-ray diffraction
C. Raman spectroscopy
D. Dielectric properties

ABSTRACT

$A_4V_2O_9$ (A = Ba, Sr, Ca, Mg and Zn) ceramics have been prepared by conventional solid state ceramic route. The phase purity of the samples was confirmed by powder X-ray diffraction technique. Raman spectroscopic studies confirm the existence of $(VO_4)^{3-}$ vibrational groups in $A_4V_2O_9$ ceramics. The possibility of existence of $A_4V_2O_9$ compositions in the AO-$V_2O_5$ binary system was also ascertained. The dielectric constant and quality factor of the ceramics under study were carried out by Hakki and Coleman post resonator and cavity perturbation techniques respectively using a vector network analyzer. Among the $A_4V_2O_9$ compositions, $Mg_4V_2O_9$ ceramic exhibits good microwave dielectric properties such as low dielectric constant of 6.3, Qxf of 37,263 GHz and negative $\tau_f$ of −43.5 ppm/°C at an optimum sintering temperature of 940 °C. Powder X-ray diffraction and EDS analyses of the co-fired $Mg_4V_2O_9$ ceramic sample show excellent chemical compatibility with Ag electrode and hence can be used as a candidate material for LTCC applications.



## 1. Introduction

The past decades have witnessed rapid advancement in modern microwave communication sectors, which necessitates the design and fabrication of miniaturized modules with better integration of electronic components and devices in multilayer ceramic structures. In order to meet these requirements, new dielectric materials with low dielectric constant for high speed signal propagation, high quality factor for increased frequency selectivity, near zero temperature coefficient of resonant frequency ($\tau_f$) for better frequency stability and low sintering temperature for the use of cheaper and highly conductive internal electrodes have been attempted. Low temperature co-fired ceramics (LTCC) have been widely used to meet the aforementioned requirements since the miniaturization of the device was of paramount importance for modern communication systems [1,2]. Even though many conventional microwave ceramics with good dielectric properties are commercially available, they are not suitable for LTCC applications owing to their high sintering temperatures [3–5]. Often low melting glasses and oxides are added to these systems to effectively reduce the sintering temperature, but this in turn deteriorates the microwave dielectric properties, especially the quality factor [6,7]. Moreover, the chemical compatibility between the dielectric ceramic and electrode material (Ag) is very important for LTCC applications [8]. Therefore, new microwave dielectric ceramics with intrinsically lower sintering temperatures, less than the melting point of Ag electrode (961 °C), have to be identified. Recently, dielectric ceramics based on low melting oxides like $TeO_2$ (732 °C), $MoO_3$ (795 °C) and $V_2O_5$ (690 °C) have been developed with promising microwave dielectric properties [9–12]. Among them, vanadate ceramics gained considerable attention owing to their excellent chemical compatibility with Ag electrode. This accelerates the search for new microwave dielectric materials based on $V_2O_5$ suitable for LTCC applications.

BaO-$V_2O_5$ phase diagram is well-studied by Fotiev et al. [13] which can be gainfully exploited for LTCC applications. According to BaO-$V_2O_5$ binary phase diagram, $BaV_2O_6$, $Ba_2V_2O_7$, $Ba_3V_2O_8$ and $Ba_3V_4O_{13}$ are stable and $BaV_{12}O_{30}$ and $BaV_8O_{21-x}$ are metastable compounds.

* Corresponding author.
*E-mail address:* ratheeshr@yahoo.com (R. Ratheesh).
[1] www.cmet.gov.in.

http://dx.doi.org/10.1016/j.materresbull.2016.12.026
0025-5408/

The metastable phases are obtained with low mole% of BaO, 10–14 mol% for $BaV_{12}O_{30}$ and 35–40 mol% for $BaV_8O_{21-x}$ respectively, whereas the stable phases $BaV_2O_6$, $Ba_2V_2O_7$, $Ba_3V_2O_8$ and $Ba_3V_4O_{13}$ are obtained with high mole% of BaO, in the range of 52–77 mol%. However, the existence of $Ba_4V_2O_9$ with higher mole% of BaO (>80 mol%), was not mentioned in the BaO-$V_2O_5$ binary phase diagram. Stable compounds in this binary system have been reported with good microwave dielectric properties such as low dielectric constant and high quality factor [14–17]. Later Golovkin and Kristallov reported the existence of $Ba_4V_2O_9$ ceramic with tetragonal crystal structure (ICDD Card No – 47-0114) in the BaO-$V_2O_5$ binary system [18]. However, no reports are available on the dielectric properties of $Ba_4V_2O_9$ ceramic.

Among the alkaline earth vanadates of general formula $A_4V_2O_9$, crystal structure of $Zn_4V_2O_9$ was well studied. Makarov et al. was the first to report the existence of $Zn_4V_2O_9$ as a compound in the ZnO-$V_2O_5$ system [19]. Clark and Pick confirmed the formation of $Zn_4V_2O_9$ and later the crystal structure is reported by Waburg and Muller [20,21]. The SrO-$V_2O_5$ binary phase diagram given by J. J. Brown confirmed the existence of $Sr_4V_2O_9$ ceramic [22]. Recently, Zhu et al. carried out the luminescent studies of $Sr_4V_2O_9$ co-doped with $Eu^{3+}$ and $Ba^{2+}$ [23]. Also, there are published reports available on the existence of $Ca_4V_2O_9$ in the CaO-$V_2O_5$ system, which exhibits close resemblance with that of $Ca_3V_2O_8$ ceramic and decomposes incongruently at a relatively higher temperature of 1365 °C [24]. However, to the best of our knowledge no reports are available on the phase formation of $Mg_4V_2O_9$ ceramic.

In the present work, we have carried out a systematic study on the structure and microwave dielectric properties of $A_4V_2O_9$ and $A_3V_2O_8$ (A = Ba, Sr, Ca, Mg and Zn) ceramics with an objective to understand the existence of $A_4V_2O_9$ ceramics in the AO-$V_2O_5$ phase diagram. The chemical compatibility of microwave dielectric systems in the $A_4V_2O_9$ (A = Ba, Sr, Ca, Mg and Zn) ceramics has also been ascertained through X-ray diffraction and EDS analyses to identify their suitability for LTCC applications.

## 2. Materials and methods

$A_4V_2O_9$ ceramics (A = Ba, Sr, Ca, Mg and Zn) were prepared by conventional solid state ceramic route. High purity oxides and carbonates such as $BaCO_3$ (Sigma Aldrich, 99%), $SrCO_3$ (Himedia, 99%), $CaCO_3$ (Sigma Aldrich, 99%), MgO (Sigma Aldrich, 99+ %), ZnO (Sigma Aldrich, 99%) and $V_2O_5$ (Sigma Aldrich, 99%) were used as starting materials. Stoichiometric amounts of the raw materials were weighed and wet mixed in distilled water for an hour in an agate mortar. The resultant slurry was dried, then ground well, and calcined at 600 °C for an hour. The calcined powders were ground again and then mixed with 5 wt% polyvinyl alcohol (PVA) as binder and dried well. The granulated powders were pressed uniaxially in a 11 mm diameter tungsten carbide (WC) die by applying a pressure of 250 MPa in a hydraulic hand press. These cylindrical green compacts were sintered in a programmable furnace at various temperatures in the range 700 °C to 1250 °C. The green compacts were fired at a rate of 5 °C/min up to the sintering temperature and an intermediate soaking was given at 600 °C for 30 min to expel the binder (PVA).

Phase purity of the $A_4V_2O_9$ samples were studied by powder X-ray diffraction (XRD) measurement using $CuK_\alpha$ radiation (Bruker 5005, Germany). The Raman spectra of the ceramic compositions under study were recorded using a Thermo Scientific DXR with Nd: $YVO_4$ DPSS laser of 532 nm. In order to study the structural resemblance of $A_4V_2O_9$ ceramics with that of alkaline orthovandates, $A_3V_2O_8$ (A = Ba, Sr, Ca, Mg and Zn) ceramics were also prepared through solid state ceramic route. All the prepared samples were calcined at 600 °C for 1 h. The sintering temperature of the samples was in the range of 700–1300 °C. The surface morphology of the sintered samples was studied using scanning electron microscopy (Zeiss, Germany). The low frequency measurements of the samples were carried out at 1 MHz using an impedance analyzer (Agilent, 4294A, Malaysia).The microwave dielectric properties were measured using a vector network

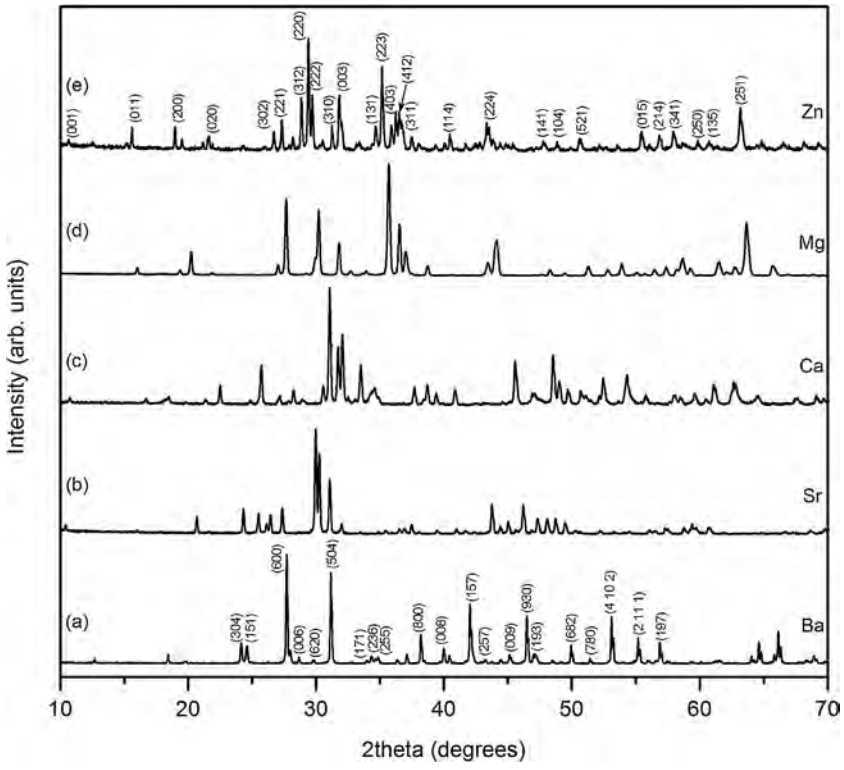


**Fig. 1.** a-e XRD patterns of $A_4V_2O_9$ (A = Ba, Sr, Ca, Mg and Zn) ceramics.

analyzer (Agilent make PNA E8362B, Bayan Lepas, Malaysia). The dielectric constant and the unloaded quality factor of the samples were measured by Hakki and Coleman post resonator and resonant cavity methods respectively [25,26]. The temperature coefficient of resonant frequency ($\tau_f$) was also measured by noting the variation of $TE_{01\delta}$ mode frequency with temperature in the range of 30–100 °C.

## 3. Results and discussion

Fig. 1a-e shows the X-ray diffraction patterns of $A_4V_2O_9$ ceramics sintered at different temperatures. Among $A_4V_2O_9$ (A = Ba, Sr, Ca, Mg and Zn) ceramics, the crystal structure of $Ba_4V_2O_9$ ceramic was studied by Golovkin and Kristallov [18]. The reported XRD pattern of $Ba_4V_2O_9$ (ICDD Card No-47-0114) is only from 20° to 60° 2theta values. The XRD pattern of $Ba_4V_2O_9$ prepared in the present study is matching with the available ICDD pattern and indexed on the basis of the same. $Ba_4V_2O_9$ ceramic crystallizes in the tetragonal system, with lattice parameters a = 18.751, and c = 18.091 Å. The calculated lattice parameters obtained for $Ba_4V_2O_9$ in the present study are a = 18.411 and c = 18.353 Å, which show good agreement with the results reported by Golovkin and Kristallov [18].

The qualitative structural analysis of $Sr_4V_2O_9$ is reported by J. J. Brown without *hkl* values and other structural parameters like space group, theoretical density etc. [22]. However, the reported d-values and intensity of XRD peaks closely matches with present study. The structural analysis of $Ca_4V_2O_9$ is reported by Y. Yuan and proposed that this composition has close resemblance with that of calcium orthovanadate [24]. Our XRD pattern of $Ca_4V_2O_9$ composition also shows close resemblance with that of orthovanadate.

On the other hand, detailed crystal structure analysis of $Zn_4V_2O_9$ is reported using Rietveld refinement by Waburg and Muller [21]. $Zn_4V_2O_9$ ceramic crystallizes in the monoclinic system, $P2_1$ space group with lattice parameters a = 10.488, b = 8.198, c = 9.682 Å and four number of molecules per unit cell ($Z = 4$). The XRD pattern obtained in the present study closely matches with that of the available reports and hence indexed accordingly (ICDD Card No-77-1757). The calculated lattice parameters of $Zn_4V_2O_9$ in the present study are a = 10.633, b = 8.013 and c = 9.601 Å which are in good agreement with the ICDD data.

In order to study the structure of $A_4V_2O_9$ ceramics in detail, Raman spectroscopic studies of these compositions were carried out. Fig. 2a-e shows the Raman spectra of $A_4V_2O_9$ ceramics and the corresponding band assignments are given in Table 1. The strong Raman bands observed in the internal mode region of $Ba_4V_2O_9$ at 832 $cm^{-1}$, 774 $cm^{-1}$ and 322 $cm^{-1}$ match with already reported Raman spectrum of $Ba_3V_2O_8$ ceramic [27]. The Raman spectra of both $Ba_3V_2O_8$ and $Ba_4V_2O_9$ show striking similarities in spite of the fact that the powder X-ray diffractions of these compositions are entirely different with different crystal structures [16]. Although the Raman spectrum of $Ba_4V_2O_9$ ceramic shows similarities with that of $Ba_3V_2O_8$ ceramics, other alkaline earth compositions in the $A_4V_2O_9$ ceramics (A = Sr, Ca, Mg and Zn) show remarkable changes in the Raman spectrum compared to $A_3V_2O_8$ analogues. The symmetry and molecular arrangements in $A_3V_2O_8$ ceramics have already been well studied and it is reported that most of these systems exhibit internal vibrations of $(VO_4)^{3-}$ groups [27,28–32].

In order to confirm the difference in the Raman spectrum of $A_4V_2O_9$ from $A_3V_2O_8$ ceramics, Raman spectra of alkaline orthovanadate ceramics were also recorded and the results are compared with that of $A_4V_2O_9$ systems (Fig. 3 and Table 2). Symmetric stretching vibrations of $(VO_4)^{3-}$ tetrahedra are observed at 859 and 848 cm-$^1$ for $Sr_3V_2O_8$ together with asymmetric stretching vibration at 779 $cm^{-1}$ whereas the

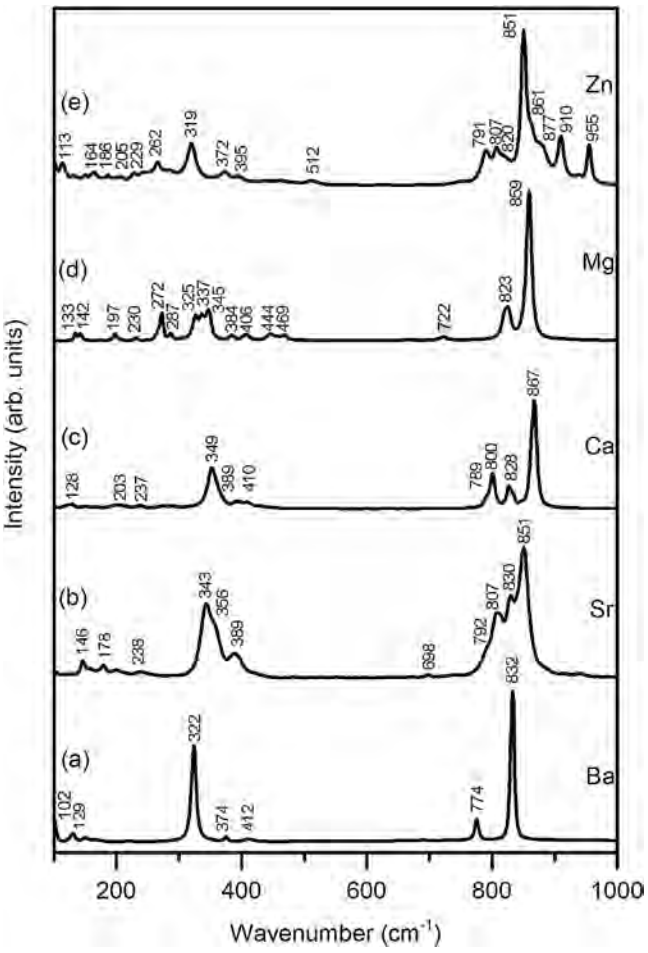


**Fig. 2.** a-e Raman spectra of $A_4V_2O_9$ (A = Ba, Sr, Ca, Mg and Zn) ceramics.

symmetric stretching vibrations of $Sr_4V_2O_9$ are appeared at 851, 830 and 807 $cm^{-1}$ together with a shoulder peak at 792 $cm^{-1}$ which can be attributed to $(VO_4)^{3-}$ asymmetric stretching

**Table 1**
Raman mode assignments of $A_4V_2O_9$ (A = Ba, Sr, Ca, Mg and Zn) ceramics.

| $Ba_4V_2O_9$ | $Sr_4V_2O_9$ | $Ca_4V_2O_9$ | $Mg_4V_2O_9$ | $Zn_4V_2O_9$ | Assignments |
|---|---|---|---|---|---|
| | | | | 955 | |
| | | | | 910 | |
| | | | | 877 | $\nu_s$ $(VO_4)^{3-}$ |
| | | 867 | 859 | 861 | |
| | 851 | | | 851 | |
| 832 | 830 | 828 | 823 | 820 | |
| | 807 | 800 | | 807 | |
| 774 | 792 | 789 | | 791 | $\nu_{as}$ $(VO_4)^{3-}$ |
| | | | 722 | | |
| | 698 | | | 512 | |
| | | | 469 | | |
| | | | 444 | | $\delta$ $(VO_4)^{3-}$ |
| 412 | | 410 | 406 | 395 | |
| 374 | 389 | 389 | 384 | 372 | |
| | 356 | 349 | 345 | | $\delta_s$ $(VO_4)^{3-}$ |
| | 343 | | 337 | | |
| 322 | | | 325 | 319 | |
| | | | 287 | | Lattice mode |
| | | | 272 | 262 | vibrations |
| | 238 | 237 | 230 | 229 | |
| | | 203 | 197 | 205 | |
| | 178 | | | 186 | |
| | 146 | | 142 | 164 | |
| 129 | | 128 | 133 | 113 | |
| 102 | | | | | |

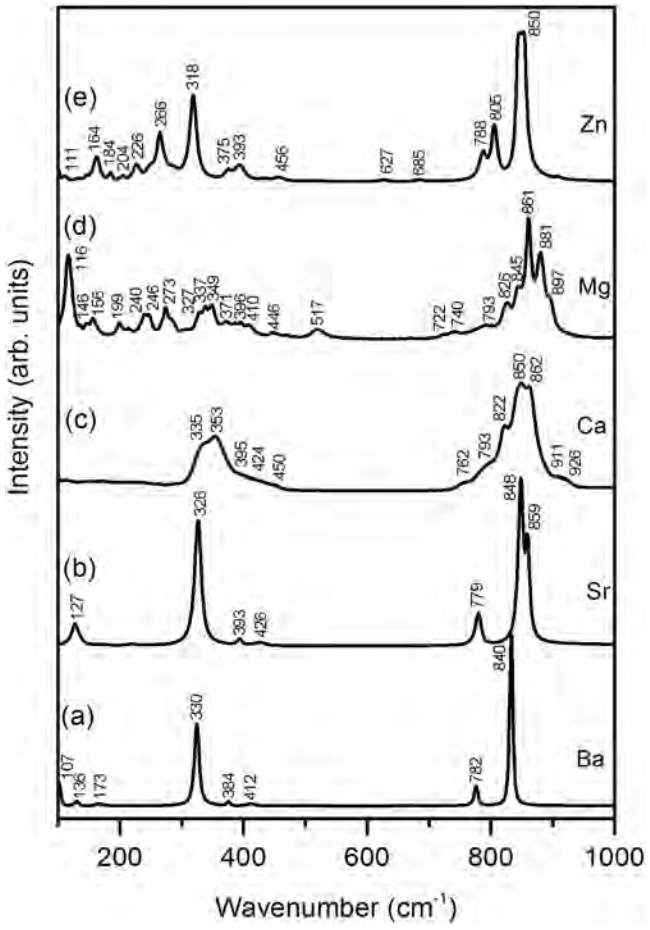


**Fig. 3.** a-e Raman spectra of $A_3V_2O_8$ (A = Ba, Sr, Ca, Mg and Zn) ceramics.

**Table 2**
Raman mode assignments of $A_3V_2O_8$ (A = Ba, Sr, Ca, Mg and Zn) ceramics.

| $Ba_3V_2O_8$ | $Sr_3V_2O_8$ | $Ca_3V_2O_8$ | $Mg_3V_2O_8$ | $Zn_3V_2O_8$ | Assignments |
|---|---|---|---|---|---|
| | | 926 | | | |
| | | 911 | | | |
| | | | 897 | | $\nu_s$ $(VO_4)^{3-}$ |
| | | | 881 | | |
| | 859 | 862 | 861 | | |
| 840 | 848 | 850 | 845 | 850 | |
| | | 822 | 826 | 805 | |
| 782 | 779 | 793 | 793 | 786 | $\nu_{as}$ $(VO_4)^{3-}$ |
| | | 762 | 740 | | |
| | | | 722 | 685 | |
| | | | 517 | 627 | |
| | | 450 | 446 | | $\delta$ $(VO_4)^{3-}$ |
| 412 | 426 | 424 | 410 | 456 | |
| 384 | 393 | 395 | 396 | 393 | |
| | | | 371 | 375 | |
| | | 353 | 349 | | |
| 330 | 326 | 335 | 337 | | $\delta_s$ $(VO_4)^{3-}$ |
| | | | 327 | 318 | |
| | | | 273 | 266 | Lattice mode vibrations |
| | | | 246 | 226 | |
| | | | 240 | 204 | |
| | | | 199 | 184 | |
| 173 | | | 156 | 164 | |
| 136 | 127 | | 146 | 146 | |
| 107 | | | 116 | 111 | |

vibrations. Similarly, the symmetric bending vibration of $Sr_3V_2O_8$ is observed at 326 $cm^{-1}$ whereas two peaks are appeared at 356 and 343 $cm^{-1}$ in the symmetric bending vibrations of $Sr_4V_2O_9$ composition. The more number of stretching and bending vibrations observed in the $Sr_4V_2O_9$ ceramic suggest a distorted $(VO_4)^{3-}$ tetrahedral arrangement for this composition compared to $Sr_3V_2O_8$ analogue.

Similar changes are observed in the Raman spectra of $Ca_4V_2O_9$ and $Mg_4V_2O_9$ ceramics. Symmetric stretching vibrations are appeared at 867, 828 and 800 $cm^{-1}$ together with asymmetric stretching vibration at 789 $cm^{-1}$ for $Ca_4V_2O_9$ compared to $Ca_3V_2O_8$ where an additional symmetric stretching mode is observed at 926 $cm^{-1}$ for $Ca_3V_2O_8$. Sharp stretching vibrations of $(VO_4)^{3-}$ are observed at 881 and 861 $cm^{-1}$ along with shoulder peaks at 897 and 845 $cm^{-1}$ for $Mg_3V_2O_8$. $Mg_4V_2O_9$ also has strong symmetric stretching vibrations at 859 and 823 $cm^{-1}$ without any shoulder peaks. Asymmetric stretching vibrations of $(VO_4)^{3-}$ groups are observed at 793, 740 and 722 $cm^{-1}$ for $Mg_3V_2O_8$ whereas only one peak is observed at 722 $cm^{-1}$ for $Mg_4V_2O_9$ ceramic. Bending and lattice mode vibrations are almost similar for both $Mg_3V_2O_8$ and $Mg_4V_2O_9$ ceramics. Also, $Mg_4V_2O_9$ has less number of peaks compared to magnesium orthovanadate.

Strong symmetric stretching vibration is observed at 850 $cm^{-1}$ for $Zn_3V_2O_8$ ceramic whereas more number of peaks is observed at 955, 910, 877, 861, 851, 820 and 807 $cm^{-1}$ for $Zn_4V_2O_9$. However, both $Zn_3V_2O_8$ and $Zn_4V_2O_9$ have almost similar symmetric and asymmetric bending vibrations compared to other alkaline earth compositions. The lower symmetry and distortion of $(VO_4)^{3-}$ tetrahedra may be the reason for the splitting of stretching modes in $Zn_4V_2O_9$ ceramics. As per the structural analysis, $Zn_3V_2O_8$ is composed of $(VO_4)^{3-}$ tetrahedra with V-O bond lengths varying from 1.67 Å to 1.79 Å whereas the V-O bond length in $(VO_4)^{3-}$ tetrahedra in $Zn_4V_2O_9$ varies from 1.65 Å to 1.84 Å. Although there

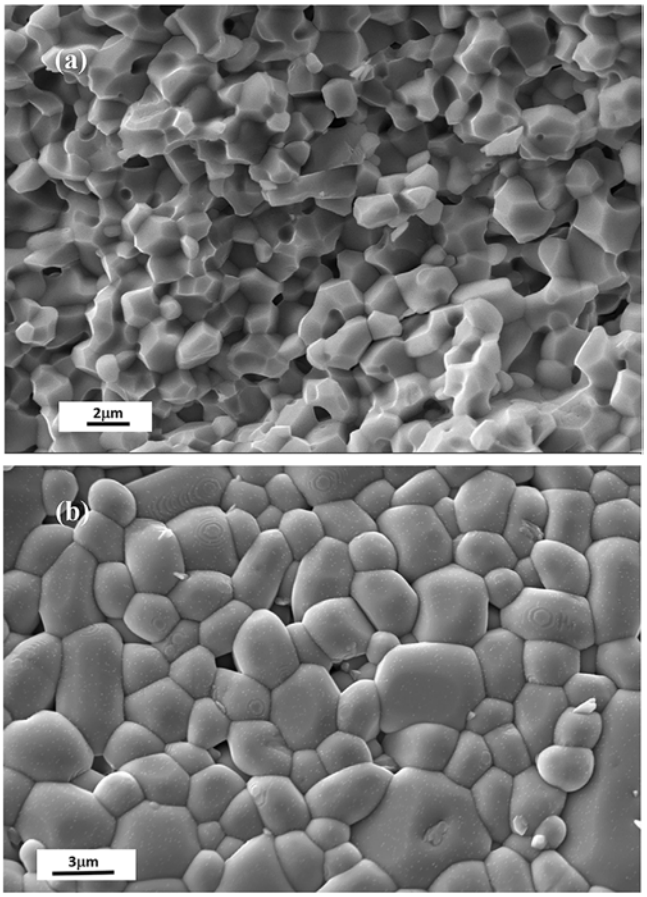


**Fig. 4.** SEM images of (a) $Ba_4V_2O_9$ sintered at 850 °C for 1 h and (b) $Mg_4V_2O_9$ at 940 °C for 1 h.

**Table 3**
Sintering temperature, density and dielectric properties of the $A_4V_2O_9$ and $A_3V_2O_8$ (A = Ba, Sr, Ca, Mg and Zn) ceramics.

| Compound | Sintering Temp. (°C) | Density (g/cc) | Low frequency data (Present study) | | High frequency data | | | References |
|---|---|---|---|---|---|---|---|---|
| | | | $\varepsilon_r$ at 1MHz | tanδ at 1MHz | $\varepsilon_r$ | Qxf (GHz) | $\tau_f$(ppm/°C) | |
| $Ba_4V_2O_9$ | 850/1 h | 4.3547 | 11.44 | 0.14 | – | – | – | This work |
| $Sr_4V_2O_9$ | 720/1 h | 3.766 | 11.16 | 0.003 | – | – | – | This work |
| $Ca_4V_2O_9$ | 1250/4 h | 2.276 | # | # | – | – | – | This work |
| $Mg_4V_2O_9$ | 940/1 h | 2.436 | 8.2 | 0.082 | 6.3 | 37,263 | −43.5 | This work |
| $Zn_4V_2O_9$ | 740/1 h | 4.141 | 18.16 | 0.1 | – | – | – | This work |
| $Ba_3V_2O_8$ | 1600/5 h | 4.5 | 13.3 | 0.094 | 11 | 62,347 | 28.8 | Ref. [16] |
| $Sr_3V_2O_8$ | 1000/1 h | 3.915 | 26.72 | 0.414 | – | – | – | This work |
| $Ca_3V_2O_8$ | 1100/1 h | 2.163 | 8.73 | 0.001 | – | – | – | This work |
| $Mg_3V_2O_8$ | 950/50 h | 3.34 | 11.4 | 0.006 | 9.1 | 64,142 | −93.2 | Ref. [33] |
| $Zn_3V_2O_8$ | 750/1 h | 4.202 | 16.17 | 0.053 | – | – | – | This work |

# Measurement not possible, - No resonance.

are not much differences in the V-O bond lengths in both the cases, the symmetric stretching vibrations of $(VO_4)^{3-}$ tetrahedra in both cases are almost differ by 105 $cm^{-1}$. In addition, an additional mode is observed at 512 $cm^{-1}$ as a weak broad band in the Raman spectrum of the later. The exact reason for such a wide variation in the symmetric stretching vibrations of $(VO_4)^{3-}$ tetrahedra in $Zn_3V_2O_8$ and $Zn_4V_2O_9$ are not clear. Further crystal structure studies are required to quantify the result.

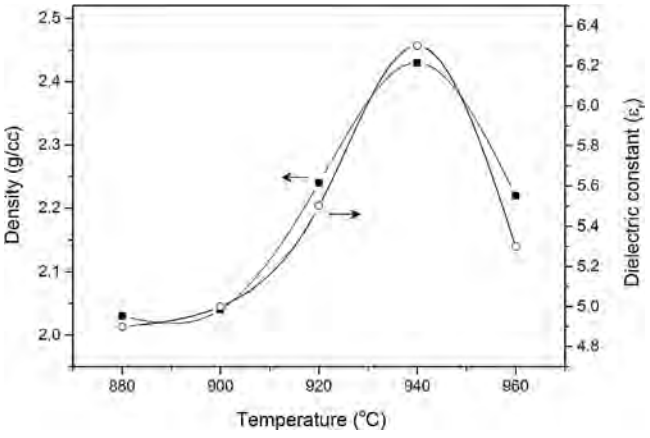


**Fig. 5.** Variation of density and dielectric constant of $Mg_4V_2O_9$ ceramic with sintering temperature.

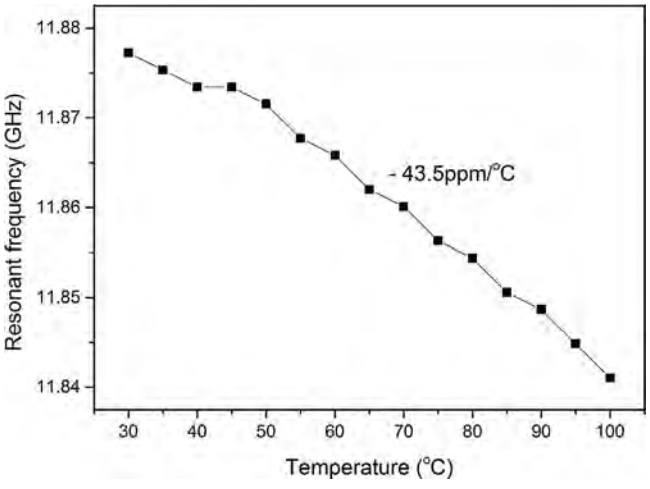


**Fig. 6.** Temperature variation of resonant frequency of $Mg_4V_2O_9$ ceramic sintered at 940 °C for 1 h.

Fig. 4 shows the SEM images of $Ba_4V_2O_9$ and $Mg_4V_2O_9$ ceramics sintered at optimum sintering temperatures of 850 °C and 940 °C for 1 h respectively. $Mg_4V_2O_9$ ceramic shows a dense microstructure with polygonal grains with 1 to 3 μm size whereas porous microstructure was observed in the SEM picture of $Ba_4V_2O_9$ ceramic.

Table 3 shows the sintering temperature, density and dielectric properties of $A_4V_2O_9$ ceramics. $A_4V_2O_9$ ceramics with A = Ba, Sr, Mg and Zn are well sintered below 950 °C but $Ca_4V_2O_9$ exhibit a maximum density of only 2.276 g/cc even after sintering at 1250 °C for 4 h. We could not measure the dielectric properties of this composition since the pellet crumbles within few hours after sintering. Among the $A_4V_2O_9$ samples studied, only $Mg_4V_2O_9$ ceramic shows microwave dielectric properties. It is clear from the Raman spectroscopic studies that among $A_4V_2O_9$, $Mg_4V_2O_9$ has least distorted $(VO_4)^{3-}$ groups, which is a clear indication of structural ordering in this composition there by resulted in better microwave dielectric properties. The optimum sintering temperature, density, dielectric constant and loss tangent of $A_4V_2O_9$ and $A_3V_2O_8$ samples at 1 MHz and GHz range are compiled in Table 3. Fig. 5 shows the variation of density and dielectric constant of $Mg_4V_2O_9$ ceramic sintered at different temperatures for 1 h. Both density and dielectric constant show an increasing trend with sintering temperature up to 940 °C. Further increase in sintering temperature deteriorates both density and dielectric constant of $Mg_4V_2O_9$ ceramics. At an optimum sintering temperature of 940 °C for 1 h, $Mg_4V_2O_9$ ceramic exhibits a maximum density of 2.436 g/cc together with a dielectric constant of 6.3 and Qxf of 37,263 GHz. Fig. 6 shows the temperature variation of resonant frequency ($\tau_f$) of

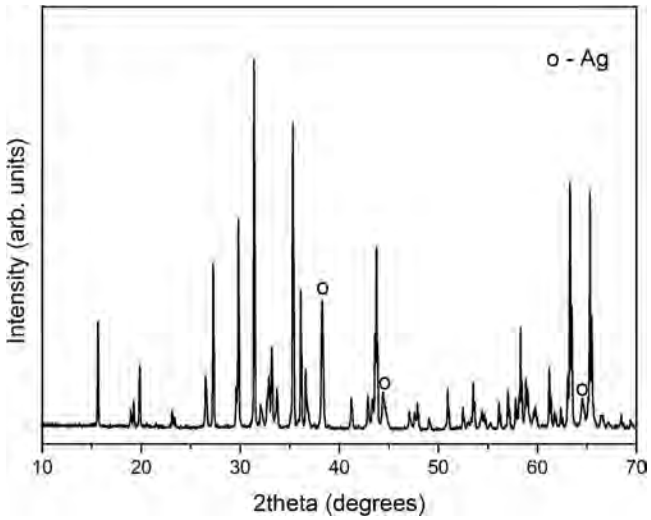


**Fig. 7.** XRD pattern of $Mg_4V_2O_9$ + 20 wt% Ag ceramic sintered at 940 °C for 1 h.

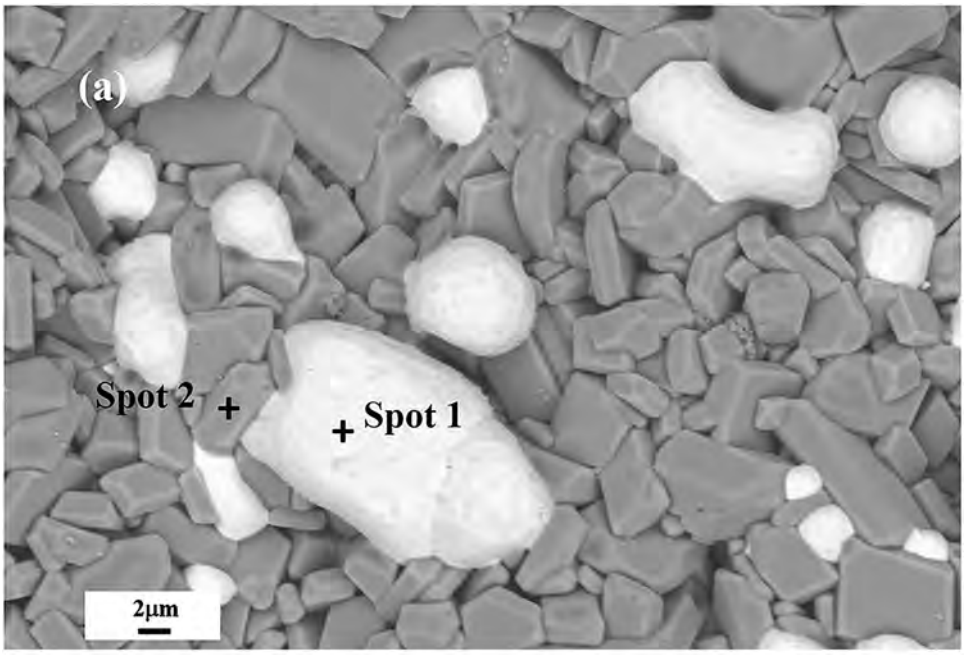


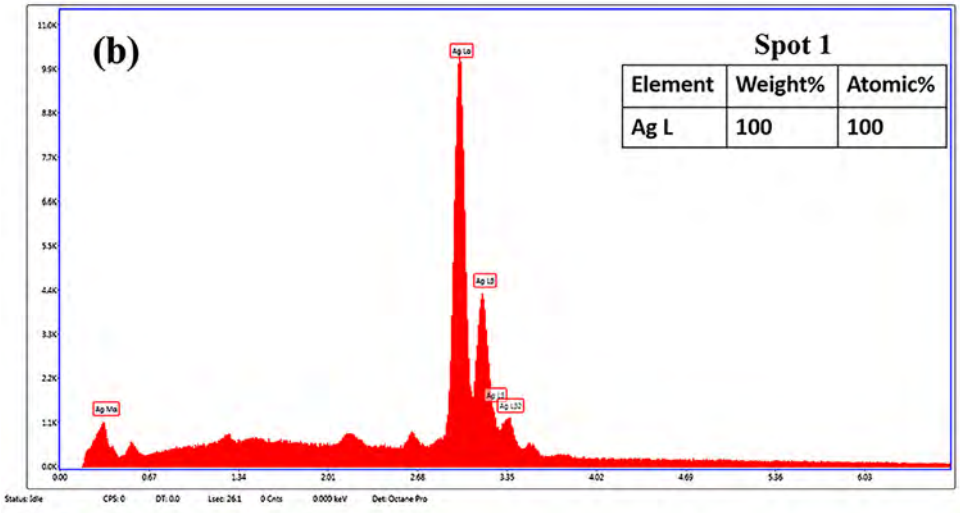


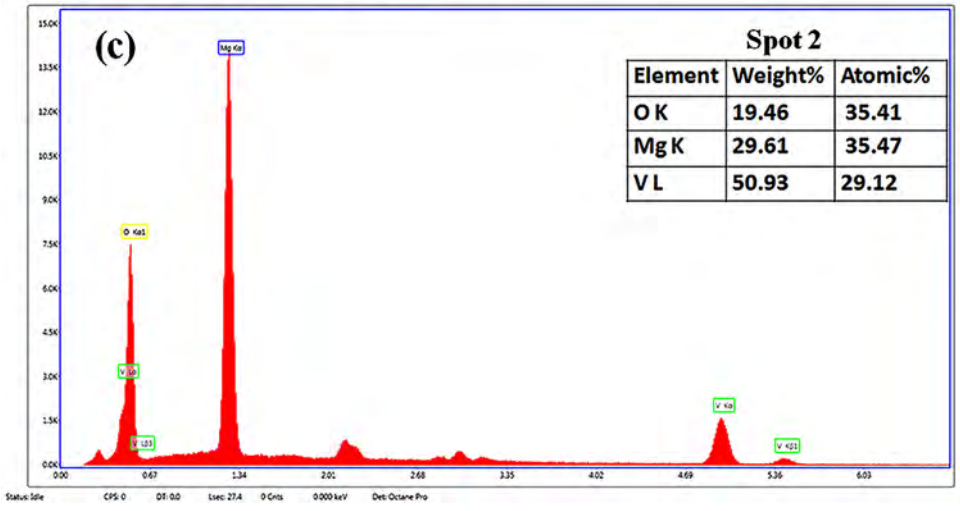


**Fig. 8.** (a) SEM image of $Mg_4V_2O_9$ ceramic co-fired with 20 wt% Ag (b) EDS spectrum of spot 1 and (c) EDS spectrum of spot 2.

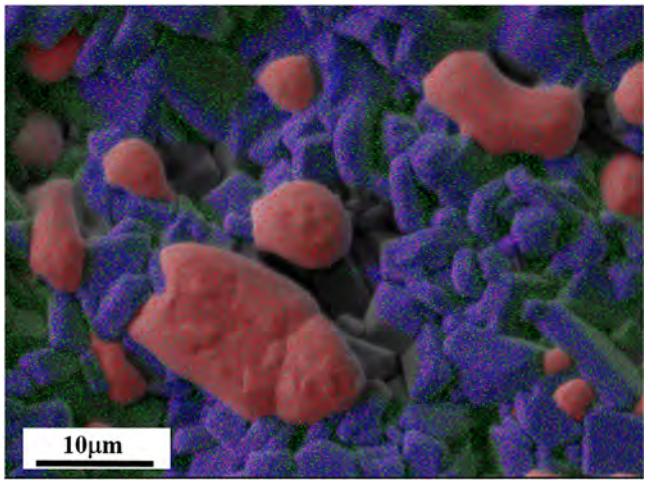


**Fig. 9.** X-ray dot mapping of $Mg_4V_2O_9$ ceramic co-fired with 20 wt% Ag.

$Mg_4V_2O_9$ ceramic sintered at 940 °C for 1 h in the range 30–100 °C. The resonant frequency of $Mg_4V_2O_9$ ceramic shows a decreasing trend with increasing temperature and the sample exhibited a negative $\tau_f$ value of −43.5 ppm/°C.

It is interesting to note that $Zn_4V_2O_9$ sample shows highest dielectric constant at 1 MHz among the samples under study. The crystal structure of this composition has the most distorted $(VO_4)^{3-}$ groups which is evident from the structural studies and the Raman bands are also observed at very high wave numbers together with splitting. The absence of microwave resonance in this composition can be attributed to the highly distorted $(VO_4)^{3-}$ groups.

In order to use $Mg_4V_2O_9$ ceramic for LTCC applications, chemical compatibility with metal electrode is an essential requirement. To evaluate the chemical compatibility, $Mg_4V_2O_9$ was co-fired with 20 wt% Ag powder at 900 °C for 1 h. The resultant XRD pattern is shown in Fig. 7 and the pattern does not show any secondary phase formation. The silver peaks are observed separately and are marked with "**o**". Fig. 8a shows the back-scattered image of the co-fired $Mg_4V_2O_9$ ceramic on the planar surface. In order to quantify the compatibility of Ag with the $Mg_4V_2O_9$ composition, co-fired samples are subjected to EDS (energy-dispersive spectroscopy) analysis (Fig. 8b and c). Spot 1 shows the segregation of melted Ag particles whereas Spot 2 represents well-formed grains of $Mg_4V_2O_9$ ceramic. It is clear from the EDS spectra that there is no inter-diffusion of Ag into $Mg_4V_2O_9$ phase. Further, the X-ray dot mapping of the co-fired sample is also done to establish the non-reactivity of Ag in the host matrix (Fig. 9). The X-ray dot mapping result clearly shows the isolation of melted Ag particles in deep red color without any inter-diffusion complementing the XRD and spot analyses results. In view of the above results, it can be inferred that the $Mg_4V_2O_9$ ceramic has excellent chemical compatibility with Ag electrode together with relatively good microwave dielectric properties and hence can be used for LTCC applications.

## 4. Conclusions

Alkaline earth vanadate $A_4V_2O_9$ ceramics with A = Ba, Sr, Ca, Mg and Zn have been prepared through conventional solid state ceramic method. The phase purity of the samples was confirmed by powder X-ray diffraction technique. Raman spectroscopic studies validated the existence of $A_4V_2O_9$ ceramics in the AO-$V_2O_5$ binary system with $(VO_4)^{3-}$ vibrational groups. Among $A_4V_2O_9$ ceramics, $Mg_4V_2O_9$ ceramic exhibits good microwave dielectric properties. At optimum sintering temperature of 940 °C for 1 h, $Mg_4V_2O_9$ ceramic has a dielectric constant of 6.3, Qxf = 37,263 GHz and a negative $\tau_f$ of −43.5 ppm/°C. The XRD and EDS analyses reveal good chemical compatibility between $Mg_4V_2O_9$ and Ag electrode. X-ray dot mapping of the co-fired $Mg_4V_2O_9$ ceramic also rule out the chemical interaction between $Mg_4V_2O_9$ and Ag powder. The present study shows that, $Mg_4V_2O_9$ ceramic can be used as a suitable candidate material for LTCC applications.

## Acknowledgements

The authors are thankful to Dr. N. Raghu, Director, C-MET, Thrissur for extending the facilities to carry out the work. The authors are also thankful to the Board of Research in Nuclear Sciences, Mumbai for financial support under grant number 34/15/01/2014-BRNS/0906.

## References

[1] M.T. Sebastian, R. Ubic, H. Jantunen, Low-loss dielectric ceramic materials and their properties, Inter. Mater. Rev. 60 (7) (2015) 392–412.
[2] Raz Muhammad, Yaseen Iqbal, Carlos Renato Rambo, Hidayatullah Khan, Research trends in microwave dielectrics and factors affecting their properties: a review, Int. J. Mater. Res. 5 (2014) 431–439.
[3] M.R. Varma, S. Biju, M.T. Sebastian, Preparation of phase pure $Ba(Zn_{1/3}Ta_{2/3})O_3$ nano powders for microwave dielectric resonator applications, J. Eur. Ceram. Soc. 26 (2006) 1903–1907.
[4] M.T. Sebastian, K.P. Surendran, Tailoring the microwave dielectric properties of $Ba(Mg_{1/3}Ta_{2/3})O_3$ ceramics, J. Eur. Ceram. Soc. 26 (2006) 1791–1799.
[5] J. Takada, S.F. Wang, S. Yoshikawa, S.J. Jang, R.E. Newnham, Effect of glass additions on $(Zr,Sn)TiO_4$ for microwave applications, J. Am. Ceram. Soc. 77 (1994) 2485–2488.
[6] C.L. Huang, K.H. Chiang, S.C. Chuang, Influence of $V_2O_5$ additions to $Ba(Mg_{1/3}Ta_{2/3})O_3$ ceramics on sintering behavior and microwave dielectric properties, Mat. Res. Bull. 39 (2004) 629–636.
[7] K.P. Surendran, P. Mohanan, M.T. Sebastian, The effect of glass additives on the microwave dielectric properties of $Ba(Mg_{1/3}Ta_{2/3})O_3$ ceramics, J. Solid State Chem. 177 (2004) 4031–4046.
[8] M. Valant, D. Suvorov, Chemical compatibility between silver electrode and low-firing binary oxide compounds: conceptual study, J. Am. Ceram. Soc. 83 (2000) 2721–2729.
[9] G. Zhang, J. Guo, L. He, D. Zhou, H. Wang, Preparation and microwave dielectric properties of ultra-low temperature sintering ceramics in $K_2O$-$MoO_3$ binary system, J. Am. Ceram. Soc. 97 (1) (2014) 241–245.
[10] W. Li, H. Xi, D. Zhou, Microwave dielectric properties of $BaY_2(MoO_4)_4$ ceramic with low sintering temperature, J. Mater. Sci. Mater. Electron. 26 (2015) 1608–1611.
[11] L. Fang, F. Xiang, C. Su, H. Zhang, A novel low firing microwave dielectric ceramic $NaCa_2Mg_2V_3O_{12}$, Ceram. Inter. 39 (2013) 9779–9783.
[12] E.K. Suresh, A.N. Unnimaya, R. Ratheesh, New vanadium based $Ba_3MV_4O_{15}$ (M = Ti and Zr) high Q ceramics for LTCC applications, Ceram. Int. 39 (2013) 3635–3639.
[13] A.A. Fotiev, V.V. Makarov, V.L. Volkov, L.L. Surat, The BaO-$V_2O_5$ system, Russ. J. Inorg. Chem. 14 (4) (1969) 144–146.
[14] A.N. Unnimaya, E.K. Suresh, R. Ratheesh, Structure and microwave dielectric properties of ultralow-temperature cofirable $BaV_2O_6$ ceramics, Eur. J. Inorg. Chem. (2015) 305–310.
[15] M.R. Joung, J.S. Kim, M.E. Song, S. Nahm, Formation process and microwave dielectric properties of the $R_2V_2O_7$ (R = Ba, Sr, Ca) ceramics, J. Am. Ceram. Soc. 92 (12) (2009) 3092–3094.
[16] R. Umemura, H. Ogawa, A. Yoko, H. Ohsato, A. Kan, Low-temperature sintering-microwave dielectric property relations in $Ba_3(VO_4)_2$ ceramic, J. Alloy. Compds. 424 (2006) 388–393.
[17] E.K. Suresh, A.N. Unnimaya, R. Ratheesh, Microwave dielectric properties of ultralow-temperature cofirable $Ba_3V_4O_{13}$ ceramics, J. Am. Ceram. Soc. 1–4 (2014).
[18] B. Golovkin, L. Kristallov, The phase composition of the BaO-$V_2O_5$ system, Zh. Nerog. Khim. 35 (1990) 253–255 [English translation Russ. J. Inorg. Chem., 35 (1990) 143].
[19] V.A. Makarov, A.A. Fotieve, L.N. Srerbryakova, Zh. Nerog Khim. 16 (1971) 2849.
[20] G.M. Clark, A.N. Pick, DTA study of the reactions of $V_2O_5$ with metal (II) oxides, J. Thermal Anal. 7 (1975) 289–300.
[21] M. Waburg, H. Muller-Buschbaum, About a new metastable compound: $Zn_4V_2O_9$, Monatsh. Chem. 117 (1986) 131–138.
[22] J.J. Brown, Phase equilibria in the system SrO-CdO-$V_2O_5$ system, J. Am. Ceram. Soc. (1972) 500–503.
[23] Y.N. Zhu, G.H. Zheng, Z.X. Dai, L.Y. Zhang, Y.Q. Li, J.J. Mu, Luminescent properties of $Sr_4V_2O_9$: $Eu^{3+}$,$Ba^{2+}$ phosphors prepared by a solvothermal method, Mater. Res. Bull. 70 (2015) 222–228.

[24] Y. Yuan, Investigation of the calcium oxide –vanadium pentoxide system, Steel Res. 62 (1991) 60–65.
[25] B.W. Hakki, P.D. Coleman, A dielectric resonator method of measuring inductive capacities in the millimeter range, IRE Trans. Mircrowave Theory Tech. (1960) 402–410 MTT-S.
[26] J. Mazierska, M.V. Jacob, A. Harring, J. Krupka, P. Barnwell, T. Sims, Measurements of loss tangent and relative permittivity of LTCC ceramics at varying temperatures and frequencies, J. Eur. Ceram. Soc. 23 (2003) 2611–2615.
[27] A.N. Unnimaya, E.K. Suresh, J. Dhanya, R. Ratheesh, Structure and microwave dielectric properties of 5BaO–2 $V_2O_5$ binary ceramic system, J. Mater. Sci. Mater. Electron. 25 (2014) 1127–1131.
[28] K.B. Shim, C.S. Lim, MAS synthesis and characterization of $Sr_3V_2O_8$ nanoparticles, J. Ceram. Proc. Research. 13 (2012) 291–295.
[29] M.K. Ryu, J.G. Choi, G.H. Kim, S. Kojima, M. Takashige, M.S. Jang, Raman scattering study in $Ca_3V_2O_8$, Ferroelectrics 332 (2006) 1–5.
[30] A. Grzechnik, High temperature tranformations in calcium orthovanadate studied with Raman scattering, Chem. Mater. 10 (1998) 1034–1040.
[31] G. Busca, G. Ricchiardi, D. Siew Hew Sam, J. Volta, Spectroscopic characterization of magnesium vanadium catalysts, part 1. vibrational characterization of $Mg_3(VO_4)_2$, $Mg_2V_2O_7$ and $MgV_2O_6$ powders, J. Chem. Soc. Faraday Trans. 90 (8) (1994) 1161–1170.
[32] S. Ni, X. Wang, G. Zhou, F. Yang, J. Wang, D. He, Crystallized $Zn_3(VO_4)_2$: synthesis, characterization and optical property, J. Alloy. Compd. 491 (2010) 378–381.
[33] R. Umemura, H. Ogawa, H. Ohsato, A. Kan, A. Yokoi, Microwave dielectric properties of low-temperature sintered $Mg_3(VO_4)_2$ ceramic, J. Eur. Ceram. Soc. 25 (2005) 2865–2870.